BOREAL ENVIRONMENT RESEARCH 19 (suppl. B): 87–107 © 2014
ISSN 1239-6095 (print) ISSN 1797-2469 (online) Helsinki 30 September 2014

Continuous flux measurements of VOCs using PTR-MS — reliability and feasibility of disjunct-eddy-covariance, surface-layer-gradient, and surface-layer-profile methods

Pekka Rantala[1,*], Risto Taipale[1], Juho Aalto[2], Maija K. Kajos[1],
Johanna Patokoski[1], Taina M. Ruuskanen[1] and Janne Rinne[1,**]

[1] *Division of Atmospheric Sciences, Department of Physics, P.O. Box 64, FI-00014 University of Helsinki, Finland (*corresponding author's e-mail pekka.a.rantala@helsinki.fi)*
[2] *Department of Forest Sciences, P.O. Box 27, FI-00014 University of Helsinki, Finland*
***current address: Department of Geosciences and Geography, P.O. Box 64, FI-00014 University of Helsinki , Finland*

Received 22 Nov. 2013, final version received 29 Jan. 2014, accepted 14 Feb. 2014

Rantala, P., Taipale, R., Aalto, J., Kajos, M. K., Patokoski, J., Ruuskanen, T. M. & Rinne, J. 2014: Continuous flux measurements of VOCs using PTR-MS — reliability and feasibility of disjunct-eddy-covariance, surface-layer-gradient, and surface-layer-profile methods. *Boreal Env. Res.* 19 (suppl. B): 87–107.

We measured VOC fluxes using disjunct-eddy-covariance (DEC), surface-layer-gradient (SLG), and surface-layer-profile (SLP) methods with proton transfer reaction mass spectrometry (PTR-MS) above a boreal forest in Hyytiälä, Finland. Our aim was to examine the reliability and feasibility of these methods for long-term measurements at low-flux conditions typical for boreal forests. The compounds targeted were formaldehyde, methanol, acetaldehyde, acetone, isoprene/methylbutenol fragment, methylbutenol, hexanal, hexenal and monoterpenes. We carried out a 10-day comparison between the techniques and used longer continuous data sets for the feasibility study. Out of these surface layer methods, the SLP method performed the best. We found out that with the SLP method we were able to detect fluxes for all the targeted compounds except formaldehyde. The method had also smaller detection limits and better data coverage than the DEC method. The systematic error of both SLP and SLG techniques was estimated to be around 10% for these measurements and it was caused by the high frequency attenuation for the DEC and by the turbulence parametrization for the SLP. As a conclusion the SLP method can be recommend for long-term flux measurements in low-flux conditions.

Introduction

Volatile organic compounds (VOCs) are mostly emitted into the atmosphere from natural sources (Guenther *et al*. 1995). Some of the compounds, such as monoterpenes, are highly reactive and their contributions to aerosol particle growth are considerable. Thus these compounds also affect the global climate system (Kulmala *et al*. 2004, 2013, Kazil *et al*. 2010). Approximately 50% of the biogenic VOC emissions originates from tropical rain forests, and the rest from other sources such as boreal forests, temperate forests, agricultural fields, and oceans (Guenther *et al*. 1995).

In order to understand seasonal and interannual changes in VOC emissions, long-term emission measurements are necessary. However, long-

Editor in charge of this article: Hannele Korhonen

term VOC emission measurements are extremely rare (Guenther *et al*. 2006, 2011). In the past decade, the disjunct-eddy-covariance method with proton transfer reaction quadrupole mass spectrometry (DEC/PTR-QMS, henceforth PTR-MS) was the method of choise for the VOC flux measurements (e.g. Rinne *et al*. 2001, 2007, Karl *et al*. 2002, Spirig *et al*. 2005, Ghirardo *et al*. 2010, Taipale *et al*. 2011). The DEC method is a direct flux measurement technique thus minimizing the sources of systematic errors. However, there are some caveats when the technique is being used for the longer-term measurements in low-flux environments. Especially the method for detection of the peak in the covariance function, needed for lag-time determination, remains a challenge (Taipale *et al*. 2010). This problem is amplified by the relatively large uncertainty caused by a limited number of samples in the disjunct-eddy-covariance method. Furthermore, the response time of the instrumentation cannot be determined using standard methods used in eddy covariance, thus complicating the correction of high-frequency attenuation.

The definition of low-flux environment is not unambiguous. In our case, this is an environment in which the flux is generally not much higher than the flux detection limit. Thus, the definition of low-flux environment does depend on the compounds of interest and our analytical and micrometeorological capabilities. With disjunct or conventional eddy-covariance techniques, environments in which the peak of the covariance function is at least an order of magnitude higher than the background noise are definitively not low-flux environments, whereas environments in which the peak in the covariance function is generally only up to two times greater the background noise can be classified as low-flux environments.

An alternative method for the determination of the VOC fluxes is the surface-layer-gradient technique (henceforth SLG) with the PTR-MS (e.g. Rinne *et al*. 2000, Spanke *et al*. 2001). In this technique, the flux F is obtained using vertical gradient of volume mixing ratios (VMR, $\overline{c}$) and turbulent exchange coefficient K analogously to molecular diffusion:

$$F = -K\frac{\partial\overline{c}}{\partial z}. \tag{1}$$

The turbulent exchange coefficient can be obtained either via the use of another scalar or via the use of the Monin-Obukhov similarity theory. In this study, we concentrate on the application of the Monin-Obukhov (MO) similarity theory (Foken 2006). With the PTR-MS, this method can potentially be applied to long-term VOC flux measurements, which is a significant extension as compared with the earlier off-line GC-MS-based applications (e.g. Rinne *et al*. 2000). The fluxes can either be derived using two measurement levels and integrated similarity functions (e.g. Fuentes *et al*. 1996, Rinne *et al*. 2000) or using measurements from several heights with a profile method (Rannik 1998). This method will be called the surface-layer-profile method (henceforth (SLP).

Our aim was to investigate the reliability and feasibility of the DEC, SLG and SLP methods for long-term measurements of ecosystem-scale VOC emissions in boreal conditions. Our three main research questions are:

1. What are the uncertainties and error sources of these methods?
2. How good data coverages are obtained by these methods in long-term measurements?
3. Do the DEC, the SLG and the SLP methods yield the same results?

To answer these questions, we present flux measurements of nine volatile organic compounds above a boreal forest obtained by all three methods. The SLG and SLP flux time series are from 1 June–31 August 2011, and the DEC flux time series from 1 June–31 August 2007. In addition, between 16 and 27 June 2011 we organized a campaign to compare the DEC and SLP.

Methods and measurements

Measurement site and VOC concentration calculations

All the measurements were conducted in Hyytiälä at the SMEAR II site (Station for Measuring Forest Ecosystem–Atmosphere Relations; 61°51´N, 24°17´E, 180 m a.m.s.l., UTC + 2) in Finland. The site is located in the boreal region and the dominant tree species is Scots pine (*Pinus sylvestris*). The forest was planted 50 years ago and the canopy height is currently about 18 m. For detailed description of the surroundings and infrastructure of SMEAR II *see* Hari and Kulmala (2005).

We used two separate PTR-MS instruments for the flux measurements, which are from now on called PTR-MS 1 and PTR-MS 2 (manufactured by Ionicon Analytik GmbH, Innsbruck, Austria in 2003 and 2008, respectively). Both are similar fast-response, high-sensitivity models (Lindinger *et al*. 1998, de Gouw and Warneke 2007).

For the DEC measurements, the sample air was transported from a 22-m-high tower to a measurement cabin and fed into the PTR-MS. The sampling tube was 32 m long, 8 mm in inner diameter, operating at a continuous flow of 17.5 l min^{-1}, and made of Teflon® (PTFE). The inlet line was heated to a few degrees above the ambient air temperature. A side flow of 0.90 l min^{-1} was taken from the inlet line to the PTR-MS via a 1.3-m PTFE tube with 1.6 mm in inner diameter. The PTR-MS was set to measure ten compounds (*see* Table 1) using a 0.5-s sampling time. The measurement frequency was ca. 1/6 Hz and the measurements were made every third hour in 2007 and continuously in 2011. PTR-MS 1 and PTR-MS 2 were used for the DEC measurements in the years 2007 and 2011, respectively. Wind and virtual temperature (T_v) were measured by an acoustic anemometer (Gill Instruments Ltd., Solent HS1199) which was located as close as possible (ca. 30 cm) to the sampling inlet.

For the profile measurements (Fig. 1), PTR-MS 1 was measuring 27 different compounds (*see* Table 1) using a 2-s sampling time

Table 1. Protonated masses measured with the DEC and the SLP/SLG system. The PTR-MS cannot separate compounds with same nominal mass and the contributing compounds listed below are the best estimates of the measured protonated masses (e.g. de Gouw & Warneke 2007).

Detected at mass (amu)	Contributing compounds	Chemical formula	SLP/SLG	DEC
31	formaldehyde	CH_2O	x	x
33	methanol	CH_4O	x	x
42	acetonitrile	C_2H_3N	x	
45	acetaldehyde	C_2H_4O	x	x
47	ethanol, formic acid	C_2H_6O	x	
59	acetone	C_3H_6O	x	x
61	acetic acid	$C_2H_4O_2$	x	
69	isoprene, methylbutenol fragment	C_5H_8	x	x
71	methacrolein, methyl vinyl ketone	C_4H_6O	x	
73	methyl ethyl ketone	C_4H_8O	x	
79	benzene	C_6H_6	x	
81	monoterpene fragments		x	x
83	methylfuran	C_5H_6O	x	
85	unknown		x	
87	methylbutenol	$C_5H_{10}O$	x	x
93	toluene	C_7H_8	x	
99	hexenal	$C_6H_{10}O$	x	x
101	hexanal	$C_6H_{12}O$	x	x
103	hexanol	$C_6H_{14}O$	x	
113	unknown		x	x
137	monoterpenes	$C_{10}H_{16}$	x	x
141	unknown		x	
153	methyl salicylate	$C_8H_8O_3$	x	
155	cineol	$C_{10}H_{18}O$	x	
169	oxidation products of monoterpenes	$C_{10}H_{16}O_2$	x	
205	sesquiterpenes	$C_{15}H_{24}$	x	
263	homosalate	$C_{16}H_{22}O_3$	x	

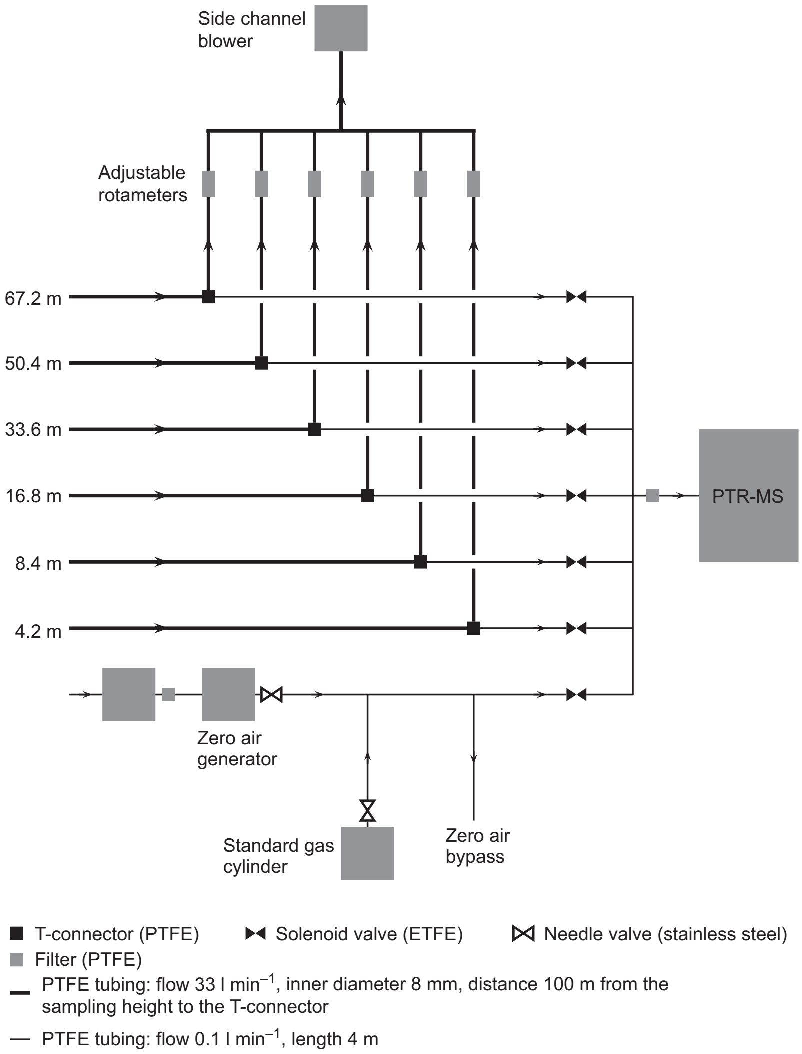

Fig. 1. The SLP and the SLG measurement setup at SMEAR II. The illustration of the DEC measurements is published elsewhere (Taipale *et al.* 2008).

from six measurement levels of a 73-m-high mast which was mounted on a protruding bedrock, ca. 2 m above the average forest floor. Two of the measurement levels (4.2 m and 8.4 m) were below the canopy level and four of them (16.8 m, 33.6 m, 50.4 m and 67.2 m) above it. The measurements were made every third hour during which PTR-MS 1 performed one minute of measurements from each level, thus a single measurement cycle covering all the measurement levels lasted six minutes, and nine full cycles were measured during one hour. The air temperature was measured with the PT-100 resistance thermometers at the height of 33.6 m, and the photosynthetic photon flux density (PPFD, Sunshine sensor BF3, Delta-T Devices Ltd., Cambridge, UK) at the height of 18 m. Carbon dioxide concentrations were measured using the URAS 4 CO_2 (Hartmann & Braun, Frankfurt am Main, Germany) at all six levels using the same sampling method and lines as for the VOCs, and the carbon dioxide fluxes were measured using Solent 1012R2 (Gill Instruments Ltd.) or LI-6262 (Li-Cor Inc., Lincoln, Nebraska) with the eddy-covariance method at the height of 23 m.

PTR-MS 1 was located inside a measurement cabin and samples were transported down to the instrument with a continuous flow of 33 l min^{-1} using a 100-m-long tubing (PTFE). From this line a side flow of 0.1 l min^{-1} was taken to PTR-MS 1 via a 4 m PTFE tube with 1.6 mm in inner diameter. A 3D acoustic anemometer (Solent 1012R2, Gill Instruments Ltd.) was installed at the height of 23 m and used for determining the friction velocities and sensible heat fluxes. Long inlet lines can potentially cause losses of the VOCs in the tubing surfaces. However, according to Kolari *et al.* (2012), a 50-m-long tubing with a flow of 1 l min^{-1} causes a loss of only a few percent of a signal as compared with a 2-m-long tubing. Thus, we can assume that the losses for the studied compounds in the present system were negligible. However, for very reactive and/or sticky compounds, such as sesquiterpenes, the tube losses can be considerable.

During the measurements, both PTR-MSs were calibrated on average every second week using a VOC standard (Apel-Riemer). The calculation procedures of VMRs are described in detail by Taipale *et al.* (2008). The instrumental background was determined every third hour by measuring the VOC-free air, produced by zero air generator (Parker ChromGas, model 3501 for PTR-MS 1; Parker ChromGas, model 1001 for PTR-MS 2).

Surface layer gradient and the profile method

The surface layer gradient method has traditionally been used to measure fluxes of compounds for which fast measurements are not available. It is based on parameterization of the atmospheric surface layer in which the turbulent transport is assumed to be analogous to molecular diffusion. Therefore, the turbulent flux of compound c, $\overline{w'c'}$, can be written as

$$\overline{w'c'} = -K_{\mathrm{h}} \frac{\partial \overline{c}}{\partial z'}, \qquad (2)$$

where K_{h} is the turbulent transfer coefficient for heat and scalars, and c is the concentration (e.g. Garrat 1994). In this work, we determined K_{h} using the MO similarity theory (Monin-Obukhov theory; Foken 2006, Monin and Obukhov 1954), in which

$$K_{\mathrm{h}} = \frac{ku_*\left(z-d\right)}{\phi_h\left(\zeta\right)}, \qquad (3)$$

where k is the von Kármán constant (we used the value 0.4; *see* e.g. Kaimal and Finnigan 1994), $\Phi_{\mathrm{h}}(\zeta)$ is the dimensionless universal stability function, and $\zeta = (z - d)/L$ is the dimensionless stability parameter where L is the Obukhov length (Obukhov 1971) and d the zero displacement height. L has been derived using dimensional analysis and it has the following form

$$L = -\frac{u_*^3 \overline{\theta}_{\mathrm{v}}}{kg\left(\overline{w'\theta_{\mathrm{v}}'}\right)_{\mathrm{s}}}, \qquad (4)$$

where

$$u_* = \left[\left(-\overline{w'u'}\right)^2 + \left(-\overline{w'v'}\right)^2\right]^{1/4}$$

is the friction velocity, θ_{v} is the potential virtual temperature, g is the acceleration due to gravity ($g \approx 9.81$ m s^{-1}), and $\left(\overline{w'\theta_{\mathrm{v}}'}\right)_{\mathrm{s}}$ is the turbulent heat transfer above the surface (in our case at 23 m). The dimensionless stability parameter ζ depends on the hydrostatic stability and $\zeta < 0$ represents unstable and $\zeta > 0$ stable conditions (e.g. Garrat 1994). The stability function $\Phi(\zeta)$ is 1 in the neutral hydrostatic stability, < 1 in unstable conditions, and > 1 in stable conditions.

When integrating Eq. 2 from a height z_1 to z_2 and assuming that $\overline{w'c'}$ remains constant, we get the following expression

$$w'c' = \frac{-ku_*\left[\overline{c}\left(z_1\right) - \overline{c}\left(z_2\right)\right]}{\ln\left(\frac{z_2-d}{z_1-d}\right) + \psi_{\mathrm{h}}\left(\zeta_1\right) - \psi_{\mathrm{h}}\left(\zeta_2\right)}, \qquad (5)$$

where ψ_{h} is the integral form of the stability function for heat (e.g. Fuentes *et al.* 1996, Rinne *et al.* 2000). With the Businger-Dyer formulations this takes the form

$$\psi_{\mathrm{h}} = 2\ln\left(\frac{1+Y}{2}\right), \zeta < 0$$

or (6)

$$\psi_{\mathrm{h}} = -\beta_{\mathrm{h}}\zeta, \zeta > 0,$$

where $Y = (1 - 12\zeta)^{1/2}$ and $\beta_{\mathrm{h}} = 7.8$ (Businger *et al.* 1971, Dyer 1974, Rannik 1998).

Equation 5 and the VMR measurements from at least two levels give us an opportunity to derive fluxes without a fast-response gas analyzer. The SLG has still several requirements for the measurement site, such as a strong horizontal homogeneity (e.g. Foken 2006). Nevertheless, the MO theory has been proven to work well at SMEAR II (Rannik 1998, Rannik *et al*. 2004). However, near the canopy top the flux gradient law tends to break down (e.g. Garrat 1980, Mölder *et al*. 1999, Simpson *et al*. 1998). The layer where the MO theory is not fully valid, is called the roughness sub-layer (RSL). In the RSL, Eq. 5 can be corrected by multiplying it by an enhancement factor, which is

$$\gamma = \frac{\overline{w'c'}}{\overline{w'c'}_{\mathrm{MO}}}, \tag{7}$$

where $\overline{w'c'}_{\mathrm{MO}}$ represents the SLG flux. Assuming scalar similarity for turbulent transport, we can use the enhancement factors obtained by e.g. CO_2 or H_2O profiles to correct the VOC fluxes derived by the SLG or SLP.

In principle, fluxes can be derived more precisely if measurements are made at several levels. The procedure is the following: According to the MO theory and assuming that the highest measurement level z_N is located above the RSL, the concentration $\bar{c}_{\mathrm{n}}$ can be derived at any height z_n using a formula

$$\bar{c}_{\mathrm{n}} = \frac{c_*}{K}\chi_{\mathrm{n}} + \dot{X}, \tag{8}$$

where

$$\chi_{\mathrm{n}} \approx \ln(z_N - d) - \psi_{\mathrm{h}}(\zeta_N) - \sum_{i=n}^{N} \frac{1}{\gamma(z_i, z_{i+1})}\left[\ln\left(\frac{z_{i+1} - d}{z_i - d}\right) - \psi_{\mathrm{h}}(\zeta_{i+1}) + \psi_{\mathrm{h}}(\zeta_i)\right]$$

and

$$\dot{X} = \bar{c}(z_0) - \frac{c_*}{k}\left[\ln(z_0) - \psi_{\mathrm{h}}\left(\frac{z_0}{L}\right)\right]$$

where χ_{n} is a normalized profile function, z_0 is the roughness length, z_N is the highest measurement level, $c_* u_* = -\overline{w'c'}$ and $N = 4$ (Rannik 1998). In hydrostatically neutral situation and without the RSL correction χ_{n} has a familiar form $\chi_{\mathrm{n}} = \ln(z_n - d)$.

Using the equations above, the surface layer parameter c_*, and the flux, can be derived using the least square estimate (a linear fit). Using only two measurement levels Eq. 8 leads naturally to the same result as the SLG (Eq. 5).

In this work, we used a constant value γ of 1.5 between the levels 16.8 m and 33.6 m. The value was determined by maximizing the mean absolute Pearson's correlation coefficient (r_{P}) between χ (Eq. 8) and CO_2 concentrations. The higher measurement levels are located typically above the RSL, thus, the corrections were not made for those levels (Rannik *et al*. 2004).

Zero displacement height

When conducting flux measurements above a forest with a canopy height, h_{c}, the zero displacement height d must often be considered. A commonly used rule of thumb estimate for d is 2/3 × h_{c} (*see* Garrat 1994). In this work, d was calculated using the method described by de Bruin and Verhoef (1997). It is based on the well-known empirical finding that under conditions of local free convection $-b_{\mathrm{w}}(z - d)/L >> 1$. Thus, d was determined as follows:

$$\sigma_{\mathrm{w}}^3 \approx C(z - d)\overline{w'\theta'}, \tag{9}$$

where $C = a_{\mathrm{w}}^3 \frac{kgb_{\mathrm{w}}}{\bar{\theta}}$, where $a_{\mathrm{w}} \approx 1.25$, $b_{\mathrm{w}} \approx 3$, and with the acoustic anemometer at the height of 23 m. Only half-an-hour periods when $-b_{\mathrm{w}}(z - d_0)/L > 10$ (we used $d_0 = 12$ m as a first approximation) were selected for the calculations. The linear fit gave $d \approx 13 \pm 1$ m (Fig. 2) which is within the uncertainty from the rule of thumb estimate of $d = 2/3 \times h_{\mathrm{r}} \approx 12$ m.

Surface layer gradient and profile flux calculations

We used the following procedure for the SLG and SLP flux calculations: First, using the PTR-MS data from 1 June to 31 August 2011 (together 616 periods) the VMRs from 16.8 m, 33.6 m, 50.4 m and 67.2 m were averaged to yield one 45-min average for every third hour (eight data points from each level). Those periods when a mean PTR-MS count rate was below the background level were disregarded. Next, we derived the friction velocities and MO lengths using the data

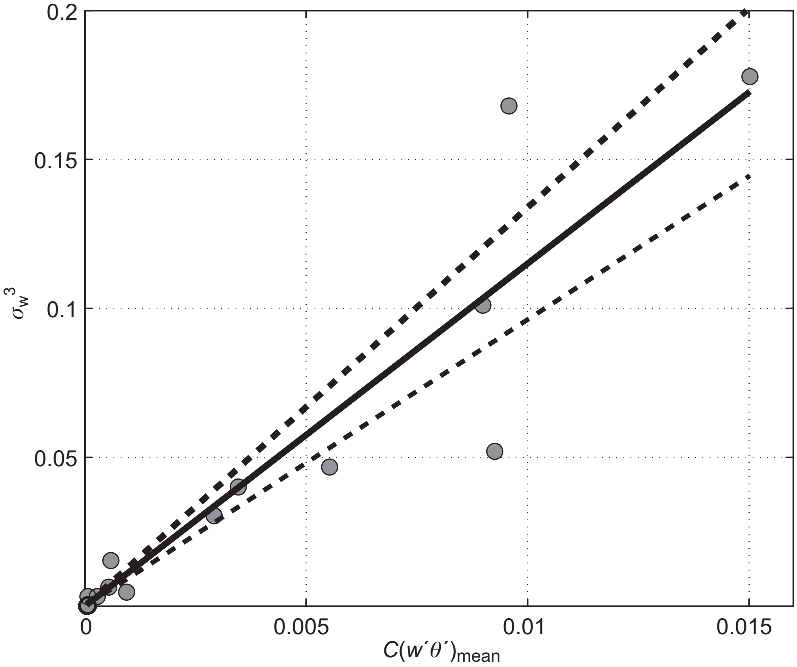

Fig. 2. σ_w^3 plotted against $C\overline{w'\theta'}$ (grey dots). σ_w represents the standard deviation of the vertical wind component and *C* is calculated using Eq. 9. The black line is a linear fit and the dashed lines are 95% confidence intervals. The slope of the fit represents the value of *z* – *d*.

from a 3D anemometer (with 2D coordinate rotation; *see* e.g. Kaimal and Finnigan 1994), and as a final step we calculated the actual profile flux values using Eq. 8 with the least-square fitting. The SLG fluxes were calculated using the VMRs from the levels 16.8 m and 33.6 m and Eq. 5. Very stable ($\zeta > 1$) and unstable ($\zeta < -2$) situations as well as the situations when $u_* < 0.2$ m s^{-1} were removed from further analysis.

Disjunct eddy covariance method

In the eddy-covariance and disjunct-eddy-covariance methods (EC and DEC, respectively), the flux is calculated using a discretized covariance:

$$\overline{w'c'} \approx \frac{1}{n}\sum_{i=1}^{n} w'\left(i - \frac{\lambda}{\Delta t}\right)c'(i), \qquad (10)$$

where *n* is the number of measurements during the flux-averaging time (typically 30–60 min), Δt is the sampling interval and λ is the lag time caused by sampling tubes (e.g. Aubinet *et al.* 2012). The EC and DEC methods are both direct flux measurement techniques, but they differ in the sampling procedure. In the EC, vertical wind and concentration fluctuations *w´* and *c´* are measured continuously using fast-response instruments, typically an acoustic anemometer and fast gas analyzer with the 10–20 Hz frequency. In the DEC, the wind component is also measured continuously with high frequency but short gas samples of 0.1–0.5 s are taken at intervals of 1–30 s (e.g. Aubinet *et al,* 2012, Rinne *et al*. 2001). Due to a long sampling interval resulting in lower number of samples used for calculation of covariances, random noise is larger in the DEC. However, this does not introduce any additional systematic error with respect to the EC (Aubinet *et al*. 2012, Lenschow *et al*. 1994).

High frequency corrections for DEC

Due to high frequency attenuation and low frequency cut-off, the measured EC or DEC fluxes do not fully correspond to the real fluxes (e.g. Moore 1986, Horst 1997). The effect of low-pass filtering can be quantified by the use of a transfer function. Formally the transfer function can be written as

$$H_{wc}(f) = \frac{C_{wc}(f)}{\overline{w'c'}_{\mathrm{ua}}} \times \frac{C_{w\theta}(f)}{\overline{w'\theta'}_{\mathrm{ua}}}, \qquad (11)$$

where C_{wc} and $C_{w\theta}$ are the co-spectra of the scalars c and w, and the scalars θ and w, respectively. $\overline{w'c'}_{\mathrm{ua}}$ and $\overline{w'\theta'}_{\mathrm{ua}}$ are un-attenuated turbulent fluxes of a scalar and temperature, respectively, and f is the frequency. A commonly used analytical form for the transfer function of a first order is

$$H_{\mathrm{wc}}(f) = [1 + (2\pi\tau f)^2]^{-1}, \qquad (12)$$

where τ is a system response time (e.g. Horst 1997).

Using the response time τ and a recursive low-pass RC filter, high frequency attenuation can be simulated using e.g. sonic temperature measurements. The attenuated sonic temperature T^{a} is

$$T_m^{\mathrm{a}} = \left(1 - e^{-\Delta t/\tau}\right) T_m + T_{m-1}^{\mathrm{a}} e^{-\Delta t/\tau}, \qquad (13)$$

where T is the real temperature, Δt a sampling interval and τ is the response time (e.g. Moore 1986). A flux correction factor α is then

$$\alpha = \frac{\overline{w'T'}}{\overline{w'T^{\mathrm{a}\prime}}}, \qquad (14)$$

We assumed the turbulence similarity, hence, the flux loss factor α was used as an approximation for VOC fluxes measured by the DEC as well. However, the flux loss factor can lead to underestimation of a flux in some cases. (Goulden *et al.* 1997, Massman and Lee 2002)

The response time for the setup of the DEC measurements was determined using high frequency water cluster (37 amu, M37) data, recorded on 4 July. This mass has the highest signal and thus gives spectra least affected by noise. The sampling interval of this data set was on average 0.245 s (range = 0.22–0.28 s). The M37 count rates were first normalized as described by Taipale *et al.* (2008). Second, the lag time between wind and the M37 measurements was estimated by maximizing the smoothed cross-covariance function of the M37 and wind measurements for every 30-min measurement period (Taipale *et al.* 2010). The wind and temperature data were also processed by choosing only the data which had been measured concurrently with the M37 and discarding the rest.

We used bin-averaged cospectra of M37 – w and θ_{v} – w to determine the values of transfer function empirically (Fig. 3; Ammann *et al.* 2006). Cospectra were calculated using the fast fourier transform. Only the clearly unstable ($\overline{w'\theta'} \geq 0.1$) and stationary (*see* Foken and Wichura 1996) 30-min periods were selected. The time constant was determined by fitting the curve described by Eq. 12 to the empirical transfer function derived using median values of calculated co-spectra (Eq. 11). This was done using the spectra data within 0.025 Hz $< f <$ 1 Hz. The higher frequencies were neglected due to the noise and the lower frequencies were found to be unattenuated.

The response time of our flux measurement system was determined to be τ = 1.2 ± 0.3 s (Fig. 3). That is similar result as compared with the response time of the PTR-MS determined by Ammann *et al.* (2006). Based on a response to artificially created step chance in signal, Karl *et al.* (2001) estimated approximately 0.8 s as the upper limit for their PTR-MS system. One should keep in mind the response time derived here depends not only on the response time of the PTR-MS but also on attenuation in the sample lines. This attenuation can be different for different compounds depending e.g. on relative humidity and their polarity which makes accurate corrections complicated for the DEC measurements (Ammann *et al.* 2006, Ibrom *et al.* 2007).

DEC flux calculations

The DEC fluxes were calculated using the VMRs from 1 June–31 August 2007 (together 596 flux periods), 3D rotated 3D-anemometer data and Eq. 10. First, we calculated cross-covariances between the vertical wind (w) and the VMRs for every 45-min measurement period and determined a lag time by maximizing the smoothed cross-covariance function from a lag time window of 0–20 s (Taipale *et al.* 2010). Finally, the fluxes were corrected using temperatures and kinematic heat fluxes measured by the sonic anemometer and the correction factor α (*see* Eqs. 13 and 14). The response time was set to τ = 1.2 s. Random uncertainties were derived

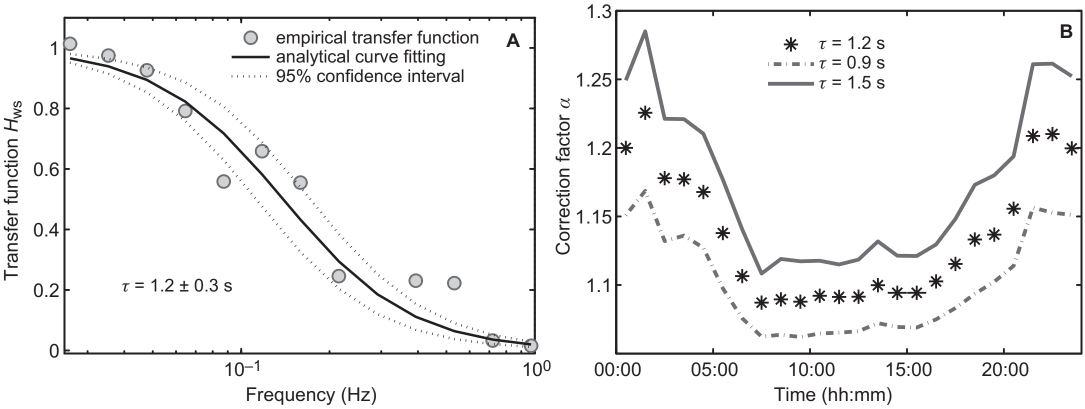

Fig. 3. (**A**) Experimental (grey dots) and analytical (black solid line) transfer functions of the water clusters measured by PTR-MS 1. (**B**) Diurnal cycle of the correction factor α using the τ values of 1.2, 1.5 and 0.9 s.

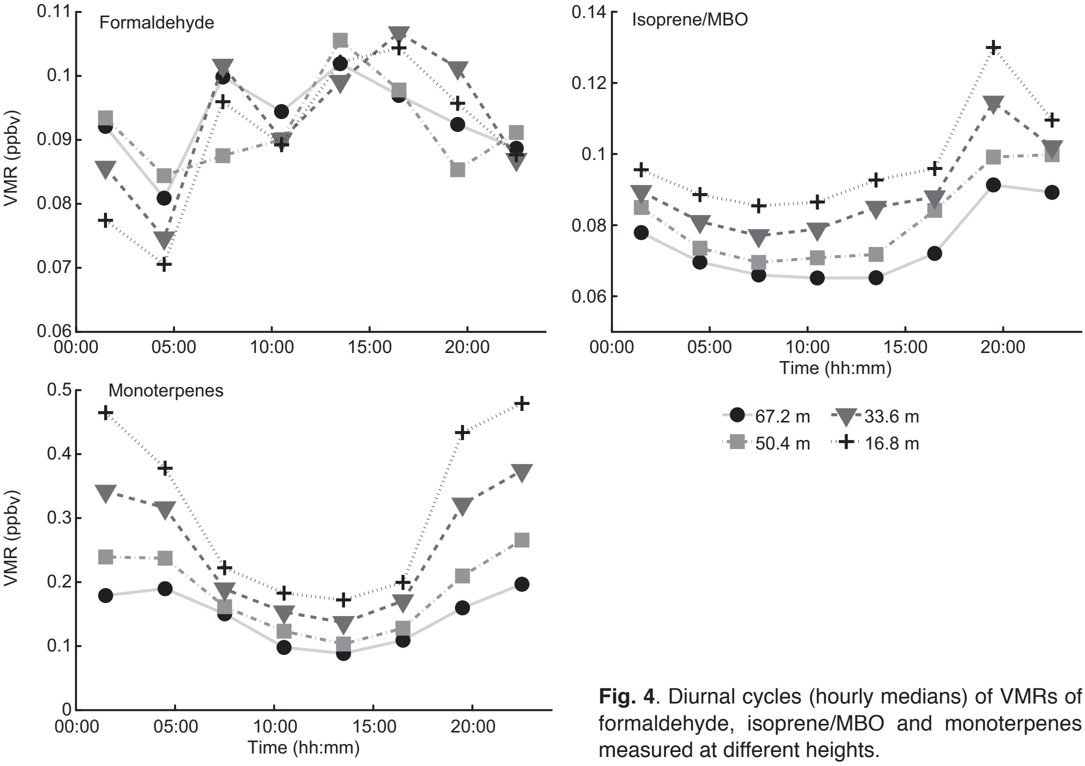

Fig. 4. Diurnal cycles (hourly medians) of VMRs of formaldehyde, isoprene/MBO and monoterpenes measured at different heights.

from the standard deviation σ_{ws} of the cross-covariance tails (Wienhold *et al*. 1994); $1.96\sigma_{ws}$ (95% CI) was used as an uncertainty as well as a flux detection limit of a single flux value (*see* Taipale *et al*. 2010). The fluxes during which u_* < 0.2 m s^{-1} were rejected from further analysis.

Results and discussion

Two examples of the median diurnal VMR cycles measured by PTR-MS 1 between 1 June and 31 August can be seen in Fig. 4. The cycle of monoterpene VMR (detected at mass 137 amu) is typical for coniferous forest sites. It can be explained by the nighttime monoterpene emissions from storage structures and by weak surface layer mixing. On the other hand, isoprene/methylbutenol fragment (henceforth isoprene/MBO, M69 amu) has a cycle peaking late in the evening because isoprene/MBO emissions are driven by sunlight (*de novo* emission) and emissions drop to zero at night. (Guenther *et al.* 1991, 1993, Ghirardo *et al.* 2010)

Data coverages, uncertainties and errors

Surface layer gradient and the profile method

Before the VOC flux calculations, validity of the SLP and SLG calculation procedures for SMEAR II during the period 16–27 June 2011 was tested using CO_2 as a tracer. First, we removed the flux data for which $u_* < 0.2$ m s^{-1} to eliminate the effect of a weak turbulence. After the filtering, the SLG and SLP gave quite similar results as compared with those given by the EC (*see* Fig. 5). The SLG fluxes were more scattered than the SLP fluxes ($r_P = 0.76$ for SLG *vs*. EC; $r_P = 0.83$ for SLP *vs*. EC; *see* Fig. 5).

A difference between the mean flux values of the SLP and EC fluxes was ca. 4%. A comparison between the SLG and SLP fluxes showed very good agreement as well, and the mean flux values differed only by 0.3% between the methods. On the other hand, the linear fit between the SLP and EC fluxes (F^{pro} and F^{ec}, respectively) gave $F^{\mathrm{pro}} = (0.9 \pm 0.05) \times F^{\mathrm{ec}} \pm 0.02$ mg m^{-2} s^{-1}, and from this we argued that the potential systematic error of the MO theory at SMEAR II is around 10%.

We also tested how well the measured VMR profiles followed the MO theory by calculating the correlation coefficient (r_P) between the measured VMRs ($\overline{c}_n$) and the normalized profile function (χ_n, Eq. 8). If the level-to-level variation in the VMR profiles was random, the distribution of r_P would be uniformly distributed between values –1 and 1. However, this holds only when the correlations are calculated using four levels, as in our SLP measurements (i.e. using two degrees of freedom; e.g. Cramér 1946). On the other hand, a distribution that consisted of correlation values of –1 (positive flux) and 1 (negative flux) alone would indicate an ideal case with non-zero fluxes and no random variation in the system.

The correlation coefficient distribution for formaldehyde was uniform (Fig. 6). Also, there were no systematic differences in the formaldehyde VMRs measured at different heights (Fig. 4). For methanol, however, the correlation coefficient distribution was non-uniform, with both positive and negative coefficient values, corresponding to both negative and positive fluxes. The distribution for monoterpenes shows that the absolute correlation coefficient was > 0.8 in over 80% of the cases. The monoterpenes also show systematic differences between VMRs measured at different heights (Fig. 4). Thus the non-uniform correlation coefficient (r_P) distribution was expected.

We can split the distributions into a uniform (random) and a non-uniform (non-random, flux related) parts, and determine a large relative fraction of each part. The fraction of non-random part represents a flux data coverage, i.e. how high percentages of derived fluxes are reliable (*see* Fig. 7 and Table 2). The friction velocity and stability filtering has also been taken into account in the results.

The importance of chemical reactions relative to turbulent mixing sources was estimated by the Damköhler number (Da) which can be formulated for the surface layer as

$$\mathrm{Da} = \frac{\tau_*}{\tau_c} = \frac{z-d}{u_* \tau_c}, \qquad (15)$$

where τ_c is the chemical life-time of a compound and $\tau_* = (z - d)/u_*$ is the time scale of the turbulent mixing (Damköhler 1940, Rinne *et al.* 2012). At SMEAR II, a typical daytime value of τ_c for α-pinene, the most abundant monoterpene in summer (Bäck *et al.* 2012, Hakola *et al.* 2012), is ca. 2 h (7000 s) (*see* Rinne *et al.* 2012) which would give Da < 0.04 at the highest measurement level of 67.2 m under the conditions of $u_* < 0.2$ m s^{-1}. According to Rinne *et al.* (2012) this causes a maximum loss of only a few percent in the monoterpene fluxes. Thus, we ignored the effect of the chemical degradation of monoterpenes. For the other compounds studied here, were

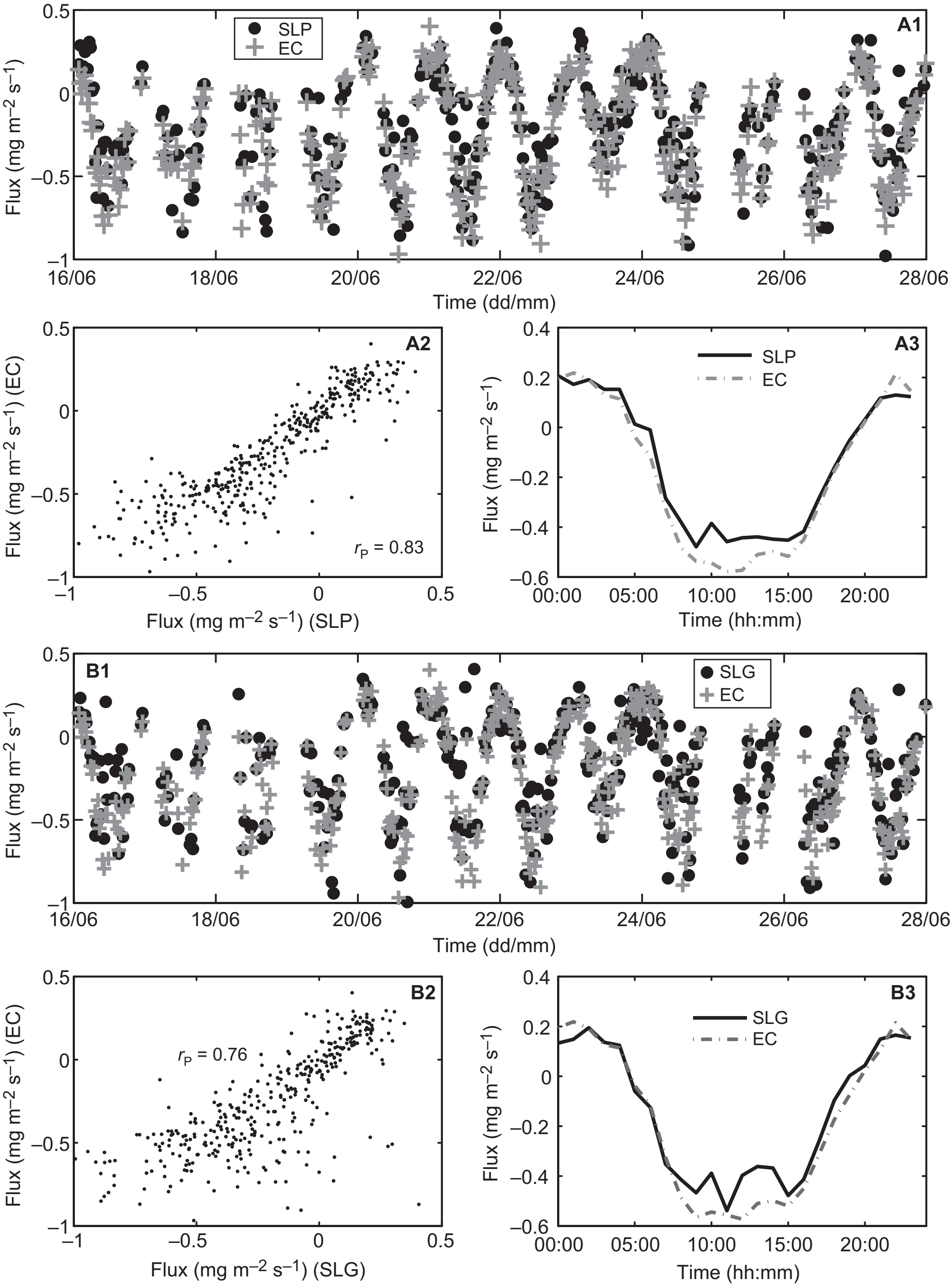

Fig. 5. Half-hourly CO$_2$ fluxes measured by the SLP, SLG and EC. (**A1** and **B1**) Time series from 16–27 June 2011 measured by the SLP and EC, and the SLG and EC, respectively. (**A2** and **B2**) Relations between the SLP and EC flux values, and the SLG and EC flux values, respectively. (**A3** and **B3**) Diurnal cycles of the SLP and EC fluxes, and the SLG and EC fluxes, respectively.

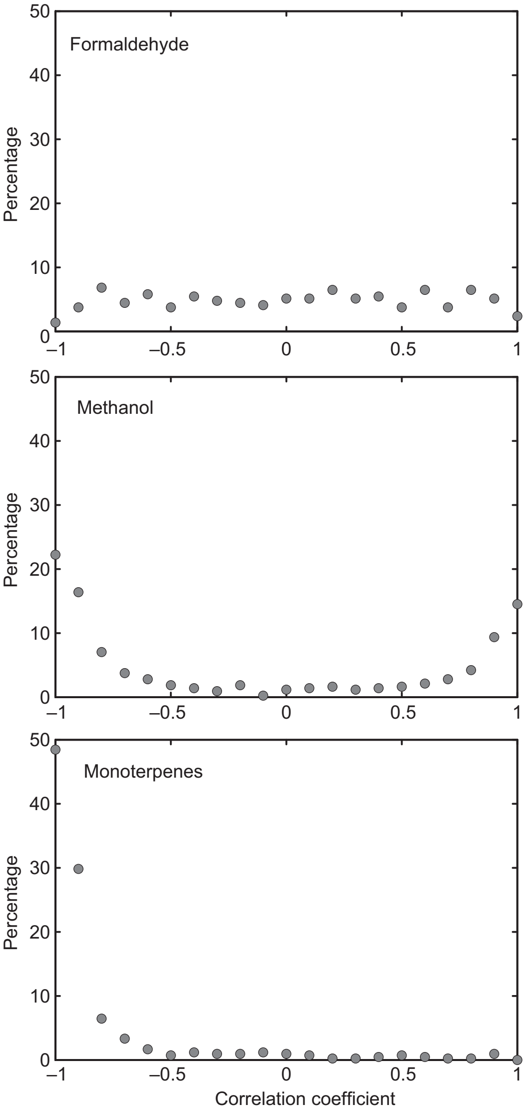

Fig. 6. The distributions of the correlation coefficients (r_P) for formaldehyde, methanol and monoterpenes. The distribution for formaldehyde is uniform, thus, there are no reliable flux values. Methanol has the U-shaped distribution, including both positive and negative fluxes. The distribution for monoterpenes is mainly composed of negative values, therefore, the derived fluxes are mainly positive.

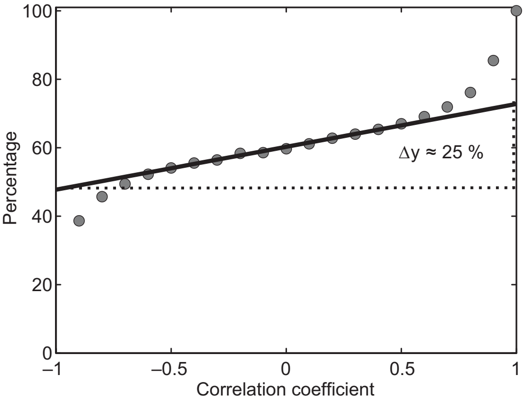

Fig. 7. Cumulative distribution of correlation coefficient (r_P) for methanol illustrating how to quantify the uniform background level Δy. First, we determined an interval where the shape of the cumulative distribution was linear. Then, a line $y(r)$ was fitted using the selected points and the linear regression. In a final step, we determined the difference $\Delta y = y(1) - y(-1)$ that describes the fraction of non-reliable flux values.

assumed similar or longer chemical life-times as that for α-pinene, thus, the effect of the chemical degradation was negligible for those compounds as well (*see* Koppman 2007: 151, Jiménez *et al*. 2007, Rinne *et al*. 2009, 2012). It should, however, be noticed that chemical sinks would have a large effect for very reactive species, such as some sesquiterpenes (Rinne *et al*. 2012).

We determined detection limits ($\mathrm{DL_{mo}}$) of the SLG and SLP fluxes as well using the equation

$$\mathrm{DL_{mo}} = \frac{\dfrac{-ku_*\mathrm{DL_{ptr}}}{\sqrt{M}}}{\ln\left[\dfrac{(z_2-d)}{(z_1-d)}\right] + \psi_\mathrm{h}(\zeta_1) - \psi_\mathrm{h}(\zeta_2)}, \tag{16}$$

where $\mathrm{DL_{ptr}}$ (95% CI) is the detection limit of a single measurement of the PTR-MS, M is the number of data points used in the calculation of the mean concentration $\bar{c}$ ($M = 8$); and z_2 and z_1 are 33.6 m and 16.8 m for the SLG, and 67.2 m and 16.8 m for the SLP. Thus, the SLP has, by definition, smaller detection limits as compared with the SLG. In this study, $\mathrm{DL_{ptr}}$ for the VMRs measured by PTR-MS was calculated by the equation

$$\mathrm{DL_{ptr}} = 1.96\sigma_\mathrm{zero},$$

where σ_zero is the standard deviation of a background measurement (Taipale *et al*. 2008). Background measurements of calibrations made between 1 June and 31 August 2011 were used for the detection limit calculations. As methylbutenol (87 amu) and hexenal (99 amu) were not included in the calibration gas-mixture, we used the detection limits of toluene (93 amu) for these compounds. For comparison, we derived also data coverages from the detection limits by requiring an absolute flux to be greater than $\mathrm{DL}_{\mathrm{mo}}$, thus $|\bar{c}(z_2) - \bar{c}(z_1)| > \mathrm{DL}_{\mathrm{ptr}}$. The data coverages of the SLP fluxes differed only by 10%–20% as compared with the data coverages calculated earlier from the correlation coefficient distributions which makes the calculated detection limits reliable. Exceptions are methybutenol, hexenal and hexanal, with detection limits that were probably underestimated.

Random uncertainties of the SLP fluxes were determined from 95% CIs of a linear regression (Eq. 8). For the SLG fluxes, we did not determine uncertainties separately. The uncertainties are large, even several hundred percent, due to a weak statistical significance of four VMR data points used to calculate gradients (Table 2).

In summary, the concentrations of methanol (33 amu), isoprene/MBO, monoterpenes, acetaldehyde (45 amu) and acetone (59 amu) followed the MO theory well. Methylbutenol, hexenal and hexanal (101 amu) had only a small non-random part. However, the detection limits for their fluxes as estimated by the SLG and SLP are still in the same range as compared with those for the other compounds. Hexanal was an exception, but its calibration was challenging, therefore, its VMRs and fluxes are probably overestimated. No reliable formaldehyde (31 amu) fluxes were detected, nevertheless, this was expected because formaldehyde is poorly detected with the PTR-MS due to its low proton affinity (de Gouw and Warneke 2007).

To test how the calculated uncertainties and errors affect the fluxes, we compared directly the fluxes measured by the SLP and SLG. The CO_2 fluxes showed that the performance of the SLG was comparable to that of the SLP but the flux values were more scattered. However, the case is more complicated for the VOCs because the VMRs of VOCs are noisier and the mean values were calculated using only eight data points. As shown earlier, this leads to large uncertainties (Table 2). Also, a small error (caused by e.g. tubing) in the VMR measurements can lead to a large error in the actual flux when only two measurement levels are used.

The average flux values of methanol, acetaldehyde, acetone, isoprene/MBO and monoterpenes produced by the SLP and SLG differed about by 10% between. For methylbutenol, hexenal and hexanal the differences were larger, up to around 100% (Fig. 8, Tables 2 and 3). Based on the correlation coefficients, the best agreement between the methods was found for methanol ($r_{\mathrm{P}} = 0.83$), isoprene/MBO ($r_{\mathrm{P}} = 0.80$) and monoterpenes ($r_{\mathrm{P}} = 0.81$). The flux footprint of the SLP is larger than that of the SLG (*see* e.g. Horst 1999), which could in part explain the observed differences. To

Table 2. Data coverages from the correlation distributions, with the detection limits for the SLG and SLP (data coverages derived from the detection limits given in parenthesis), and uncertainties for the profile method. r_{P} is the Pearson correlation coefficient and *a* and *b* (ng m^{-2} s^{-1}) are the parameters of the linear fit $F_{\mathrm{gra}} = F_{\mathrm{pro}}a + b$, where F_{pro} is the SLP flux and F_{gra} is the SLG flux. $\mathrm{DL}_{\mathrm{gra}}$, the $\mathrm{DL}_{\mathrm{pro}}$, U_{pro} and *b* have the unit of ng m^{-2} s^{-1}.

Compound	Data coverage (%)	Detection limits* (ng m^{-2} s^{-1})		Uncertainties* profile method (ng m^{-2} s^{-1})	r_{P} (*n*)	*a* (±95% CI)	*b* (±95% CI)
		SLG	SLP				
Formaldehyde	0	–	–	–	–	–	–
Methanol	52	6–23 (42%)	2–10 (59%)	10–76	0.83 (407)	1.0 ± 0.05	–3 ± 3
Acetaldehyde	39	3–11 (26%)	0.9–5 (44%)	2–23	0.61 (407)	0.9 ± 0.1	–4 ± 2
Acetone	42	2–9 (46%)	0.7–4 (61%)	3–33	0.60 (407)	0.9 ± 0.1	–4 ± 2
Isoprene/MBO	48	1–4 (45%)	0.5–2 (56%)	1–18	0.80 (379)	1.0 ± 0.1	–2 ± 1
Methylbutenol	21	2–7 (21%)	0.6–3 (63%)	1–11	0.58 (380)	1.0 ± 0.2	0 ± 1
Hexenal	16	2–7 (61%)	0.6–3 (70%)	1–11	0.58 (381)	1.3 ± 0.2	1 ± 1
Hexanal	22	23–88 (29%)	7–40 (49%)	16–190	0.69 (383)	1.6 ± 0.2	0 ± 35
Monoterpenes	62	2–6 (63%)	0.5–3 (68%)	5–37	0.81 (399)	0.9 ± 0.1	0 ± 10

* 25–75 percentiles.

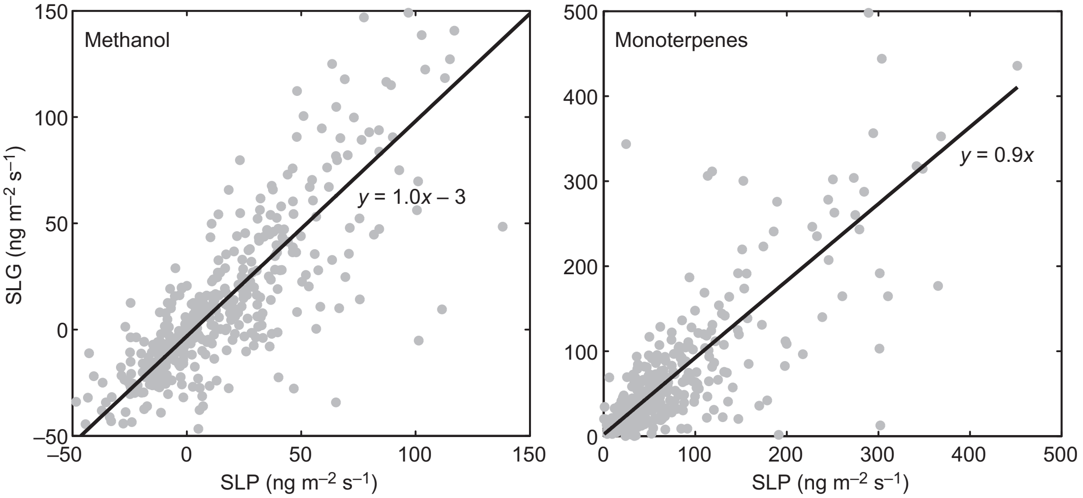

Fig. 8. Fits between the SLP and SLG fluxes of methanol and monoterpenes. Negative monoterpene fluxes were rejected from the analysis

examine this, we studied whether the differences between the SLG and SLP fluxes depend on wind directions. Although some differences between the methods were a function of wind direction, no systematic behavior was observed. Thus, no filtering based on the wind direction was done.

Disjunct-eddy-covariance method

To quantify quality of the DEC fluxes at SMEAR II, we analysed flux data from the period 1 June–31 August 2007. Using the detection limits of the DEC we determined the data coverage after all flux values lower than the detection limit were rejected. With this method we obtained data coverages of around 30% for random data, calculated from the cross covariance functions far from the peak. This indicates an inherent problem with the approach in which we select (i) the maximum covariance peak for a given time window and connect this to the flux, and (ii) the detection limit determined via the standard deviation of the covariance function well away from the peak (Table 4; Wienhold *et al*. 1994).

Table 3. Average fluxes measured estimated by the SLG and SLP ($\bar{F}_{\mathrm{gra}}$ and $\bar{F}_{\mathrm{pro}}$, respectively) and the ratios between them. The averages were calculated using only positive flux values. The unit is ng m^{-2} s^{-1}.

Compound	$\bar{F}_{\mathrm{gra}}$	$\bar{F}_{\mathrm{pro}}$	$\bar{F}_{\mathrm{gra}}/\bar{F}_{\mathrm{pro}}$
Formaldehyde	–	–	–
Methanol	43.9	40.8	1.08
Acetaldehyde	11.0	9.4	1.17
Acetone	19.7	18.8	1.05
Isoprene/MBO	14.1	12.9	1.10
Methylbutenol	10.2	5.55	1.84
Hexenal	11.5	5.78	1.99
Hexanal	252	125	2.01
Monoterpenes	72.3	78.4	0.92

Depending on the selected confidence interval and the lag-time window there is a statistical likelihood that the highest values of the covariance function of random data exceed the detection limit. Thus the selection of the highest value of the covariance function will lead to fluxes that artificially exceed the detection limit. The artifact data coverages show e.g. 31% coverage for formaldehyde (Table 4), even though the coverage should be 0%. From this we estimated that the data coverages of the DEC were in reality smaller than the corresponding data coverages of the SLP.

Systematic errors of the DEC fluxes due to uncertainty in high-frequency correction were derived using the 95% confidence intervals of the response time τ. Due to the scatter in the data, the correction factor can vary about 10% and it causes a systematic uncertainty of ca. 10%

(Table 4). This error was of the same magnitude as the estimated systematic error of the MO theory.

The comparison between the surface layer profile and disjunct eddy covariance method

As we have shown evidence above for the SLP fluxes being more reliable than the SLG fluxes. Below, we compare the SLP and DEC fluxes using the calculated flux values from the periods 1 June–31 August 2011 and 1 June–31 August 2007, respectively. Even though the fluxes were not measured concurrently, the comparison gives information whether the fluxes are comparable and how well they capture the general flux patterns. The diurnal behaviour was quite similar and the flux values were within the same order of magnitude for all VOCs (Fig. 9, Tables 3 and 4). A remarkable result is that the DEC flux values were much more scattered than the SLP flux values. It is e.g. generally known that isoprene has a clear diurnal cycle and emissions are light- and temperature-dependent, decreasing to zero at sunset. However, 35% and 65% percentiles of the DEC flux values showed large variations at all hours whereas the comparable percentiles of the SLP flux values decreased to zero by night as they should. Those percentiles were selected because 25% and 75% quartiles would have produced unclear figures due to the large scatter of the DEC fluxes.

The results discussed above also show that the DEC technique has greater detection limits and smaller data coverages than the SLP technique. On the other hand, calculated uncertainties of the SLP technique for methanol, acetaldehyde, acetone, isoprene/MBO and hexanal fluxes (Tables 2 and 4) were greater than the corresponding uncertainties of the DEC technique. The diurnal cycles, however, show more scatter in the DEC fluxes. Thus, it seems that either the uncertainties of the SLP fluxes are overestimated or the uncertainties of the DEC fluxes are underestimated.

We also performed a direct comparison between the DEC and the SLP using a data set from 16–27 June 2011. The comparison was made only for methanol and monoterpene fluxes because of instrumental problems of PTR-MS 2 in the VMR measurements of other compounds during the period. The correlation coefficients between hourly-averaged VMRs measured simultaneously by PTR-MS 1 and PTR-MS 2 were 0.80 and 0.77 for methanol and monoterpenes, respectively, whereas for the other compounds the correlation coefficients were less than 0.40. There was also a systematic difference in methanol calibration with the two systems, thus the DEC fluxes of methanol were scaled by a factor of

$$\eta = \frac{\overline{\mathrm{M33}_{\mathrm{pro}}}}{\overline{\mathrm{M33}_{\mathrm{dec}}}}, \tag{17}$$

where $\overline{\mathrm{M33}_{\mathrm{pro}}}$ and $\overline{\mathrm{M33}_{\mathrm{dec}}}$ are the mean values of methanol VMR of the PTR-MS 1 (an average

Table 4. Data coverages and detection limits (25–75 percentiles) for the DEC. R is the effect of the high frequency correction as a function of τ (τ = 0.9 – 1.5 s) such that with the value τ = 1.2 s the average flux is scaled to 1. $\overline{F}_{\mathrm{dec}}$ is the mean flux derived from positive DEC flux values.

Compound	Data coverage (%)	*Data coverage calculated from random noise (%)	Detection limits* (ng m^{-2} s^{-1})	$\overline{F}_{\mathrm{dec}}$ (ng m^{-2} s^{-1})	R*
Formaldehyde	30	31	3–7	–	–
Methanol	49	36	8–20	33.2	0.98–1.04
Acetaldehyde	36	31	3–8	9.4	0.94–1.04
Acetone	45	33	7–16	20.4	0.97–1.03
Isoprene/MBO	40	32	5–11	12.9	0.96–1.04
Methylbutenol	35	32	4–10	10.4	0.93–1.06
Hexenal	36	33	6–13	14.0	0.96–1.04
Hexanal	34	32	28–88	81.9	0.95–1.05
Monoterpenes	57	34	17–37	59.8	0.97–1.04

* Detection limits also represent uncertainties of the DEC.

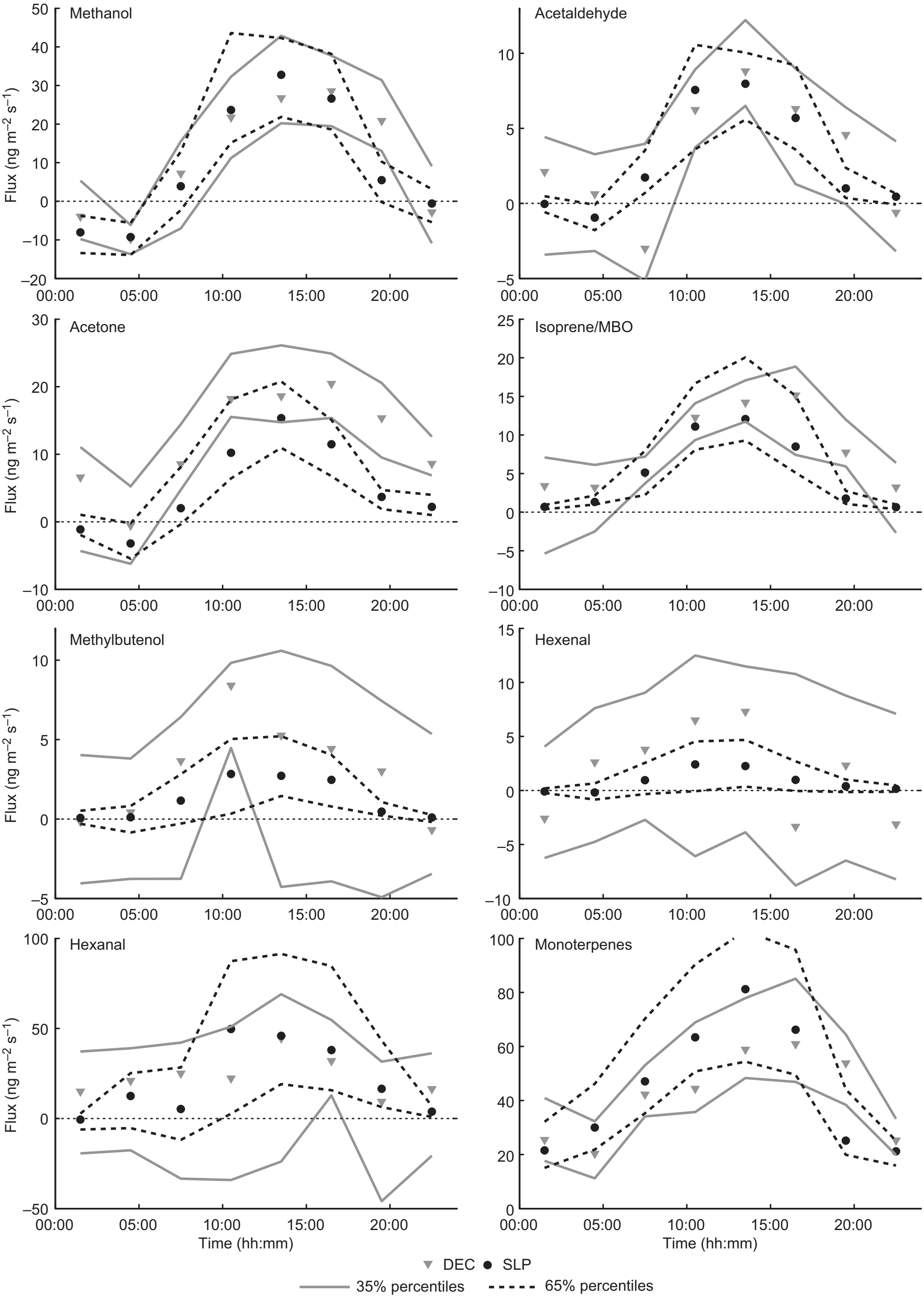

Fig. 9. Diurnal cycles (hourly medians) of methanol, acetaldehyde, acetone, isoprene/MBO, methylbutenol, hexenal, hexanal and monoterpene fluxes (1 June–31 August 2011 for SLP; 1 June–31 August 2007 for DEC).

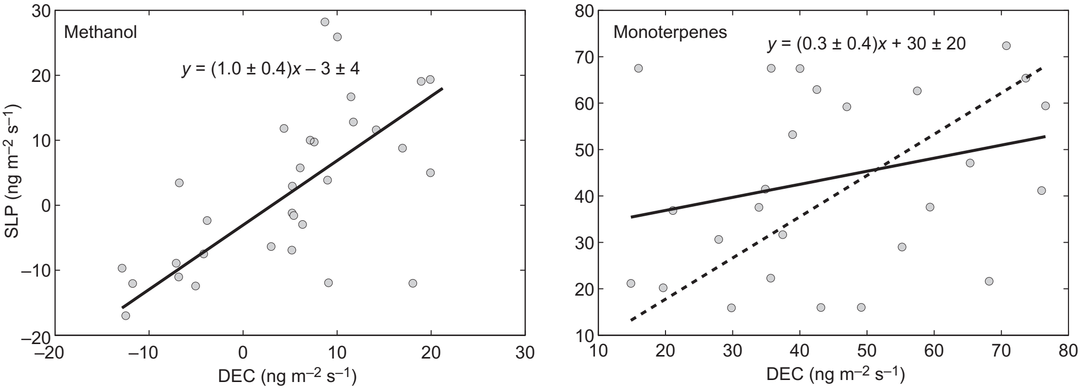

Fig. 10. SLP fluxes against DEC fluxes for methanol and monoterpenes. The grey dots show the measurements and the black solid lines the linear fits. The dashed line in the right panel shows the linear fit forced through the origin.

from the levels 16.8 m and 33.6 m) and PTR-MS 2 measurements, respectively. From the comparison we removed 10% of the largest absolute flux values as well as negative values of monoterpene fluxes. Even though the data sets are relatively small, the methanol fluxes were consistent between the methods (Fig. 10): $r_P = 0.71$, $p < 10^{-5}$ ($n = 34$) and the slope of the linear fit 1.0. No correlation for monoterpenes was found ($n = 27$, $p = 0.20$). The offset was also large (30 ng m^{-2} s^{-1}). If the line was forced to go through the origin, the slope was far better (0.89).

From the comparison above we are only able to state that monoterpene fluxes obtained with the two techniques do not correlate well, but not which one is more trustworthy. In order to assess which method yields fluxes corresponding better to our prior understanding on the BVOC emissions we compared the fluxes of isoprene/MBO and monoterpenes with the emission algorithms for these compounds. We chose these two compounds for comparison as their emission algorithms are based on understanding of emission mechanisms, rather than being fully empirical (e.g. Guenther *et al.* 1991 or Guenther *et al.* 1993).

The well-known algorithm for isoprene emissions (E) is

$$E = E_{\mathrm{synth}} = E_{0,\mathrm{synth}} C_{\mathrm{T}} C_{\mathrm{L}}, \qquad (18)$$

where $E_{0,\mathrm{synth}}$, C_{T} and C_{L} are same as in the traditional synthesis algorithm (*see* Guenther *et al.* 1991, 1993). The shape of this algorithm is based on the light response curve of electron transport activity and the temperature dependence of the protein activity. The algorithm we use for monoterpene emissions is the following hybrid algorithm:

$$E = E_{\mathrm{synth}} + E_{\mathrm{pool}} = E_0[f_{\mathrm{synth}} C_{\mathrm{T}} C_{\mathrm{L}} + (1 - f_{\mathrm{synth}})\Gamma], \qquad (19)$$

where $f_{\mathrm{synth}} = E_{0,\mathrm{synth}}/E_0$ (Ghirardo *et al.* 2010, Taipale *et al.* 2011), E_{pool} is the traditional pool algorithm from Guenther *et al.* (1991, 1993), and Γ is the temperature activity factor. This algorithm is based on the finding that part of the monoterpene emission from coniferous trees originates directly from synthesis, hence, it can be calculated using algorithm similar to isoprene emission algorithm. The rest is evaporation from large storage pools (Ghirardo *et al.* 2010), which can be calculated using exponentially temperature-dependent algorithm, as the temperature dependence of the monoterpene saturation vapour pressure is approximately exponential (Guenther *et al.* 1991, 1993). Thus, we investigate which one of the flux measurement methods agrees better with our prior understanding of the diurnal scale variation of the emissions. The parameters C_{T}, C_{L} and Γ were taken from Guenther (1997). Thus, the only free parameter of the synthesis algorithm was the emission potential E_0, whereas in the hybrid algorithm also f_{synth} is a free parameter. The isoprene/MBO and monoterpene fluxes, measured with the SLP and DEC methods in July 2011 and July 2007, respectively, were fitted against the emissions calculated using the algo-

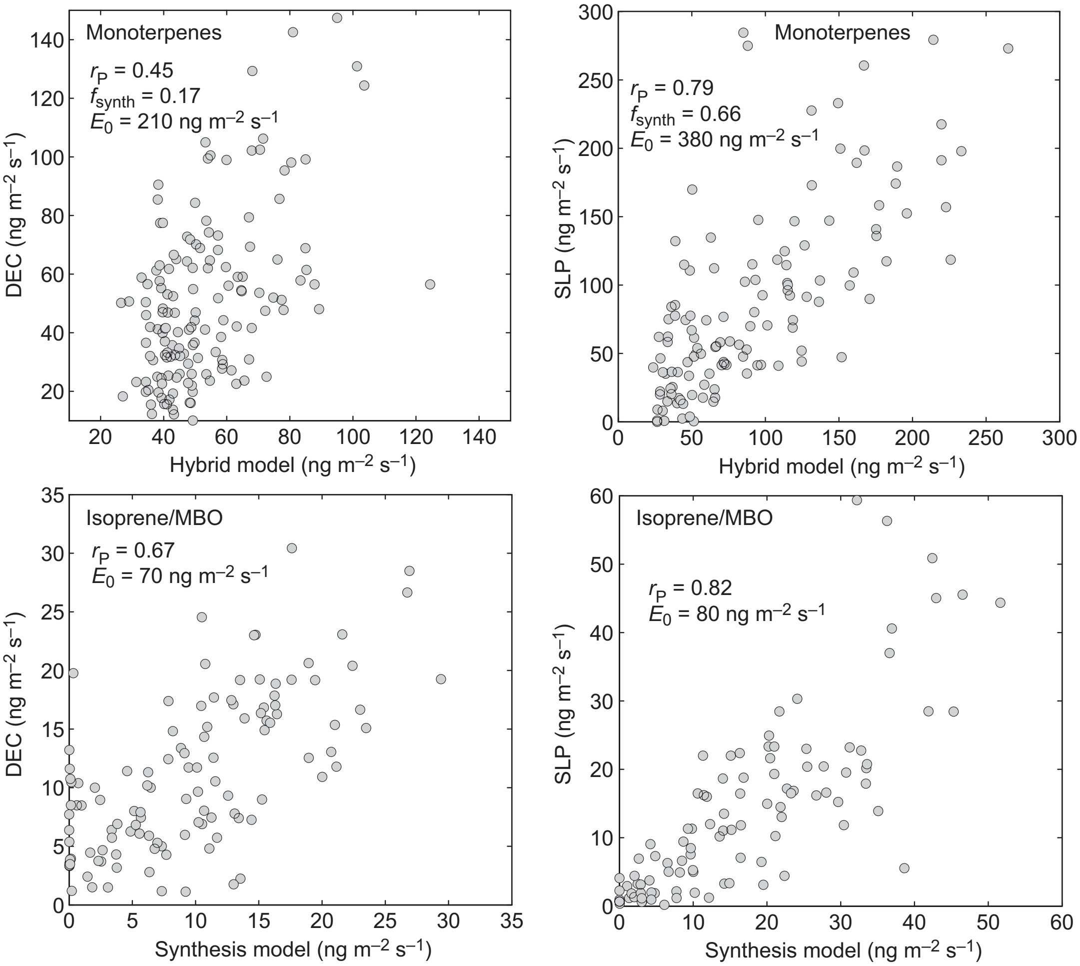

Fig. 11. Measured monoterpene and isoprene/MBO fluxes against the emissions calculated by the emission algorithms with linear fits.

rithms. Negative flux values were rejected from the analysis.

The SLP method correlated better than the DEC method with the results produced by both emission algorithms (Fig. 11). This indicates that, if we trust these emission algorithms to describe the short-term variations in isoprene and monoterpenes adequately, the SLP method seems to be more reliable than the DEC method. Furthermore, it is interesting to note that despite the differences in the correlations between the flux measurement techniques and the calculated emissions, the standard emission potential of isoprene derived from the DEC and SLP fluxes is essentially the same. For monoterpenes those are not as similar but still less than a factor of 2 apart.

Conclusions

The VOC flux measurements with the PTR-MS in the northern boreal environment have proven to be a challenging task due to the relatively low emissions and concentrations, especially if long time-series are targeted. However, we have shown that the use of the surface-layer-profile (SLP) method connected with the Monin-Obukhov similarity theory provided a feasible solution for the long-term flux measurements in these conditions. The comparisons showed that the magnitudes of all studied fluxes measured by the SLP and the surface-layer-gradient (SLG) methods were on average the same as those measured by the disjunct-eddy-covariance

(DEC) method. In addition, the simultaneous comparison of the DEC and SLP showed good agreement for methanol as well, although the monoterpene fluxes compared less satisfactorily. The SLP had smaller detection limits than the DEC and it was also less sensitive to the instrumental noise or tube attenuation. Therefore, we can recommend the use of the SLP for long-term flux measurements in low-flux conditions. Especially, if the possible effect of the surface roughness layer can be quantified and corrected.

In principle, the DEC is a direct method and therefore it is less prone to systematic errors. Thus, the first choice for quantifying the ecosystem scale VOC fluxes. However, in low-flux conditions the technique has large random errors leading to high detection limit. Also, with the reduced amount of the data used to calculate the covariance function makes the determination of the lag-time challenging. The standard approach to selecting the maximum of covariance function and associating it with the flux in a given time window can also lead to systematic overestimation of absolute flux values. Long inlet lines can also be a cause if systematic errors in the flux measurements, but they seem to be quite small. In conditions with higher fluxes the situation is of course different and the use of the DEC is well justified.

Acknowledgements: We acknowledge the support from the Academy of Finland through its Centre of Excellence program (1118615) and other projects (125238, 140778). We also thank E. Siivola, J. Levula, R. Pilkottu and other Hyytiälä personnel for contributing to the data collection. V. Hemmilä is acknowledged for his help with the data analysis.

References

Ammann C., Brunner A., Spirig C. & Neftel A. 2006. Technical note: water vapour concentration and flux measurements with PTR-MS. *Atmospheric Chemistry and Physics* 6: 4643–4651.

Aubinet M., Vesala T. & Papale D. 2012. *Eddy covariance: A practical guide to measurement and data analysis*. Springer Atmospheric Sciences, Springer, Dordrecht, Heidelberg, London, New York.

Bäck J., Aalto J., Henriksson M., Hakola H., He Q. & Boy M. 2012. Chemodiversity of a scots pine stand and implications for terpene air concentrations. *Biogeosciences* 9: 689–702.

Businger J.A., Wyngaard J.C., Izumi Y. & Bradley E.F. 1971. Flux-profile relationships in the atmospheric surface layer. *Journal of the Atmospheric Sciences* 28: 181–189.

Cramér H. 1946. *Mathematical methods of statistics*. Princeton University Press, Princeton.

Damköhler G. 1940. Der Einfluss der Turbulenz auf die Flammengeschwindigkeit in Gasgemischen. *Zeitschrift für Elektrochemie und Angewandte Physikalische Chemie* 40: 601–652.

De Bruin H.A.R. & Verhoef A. 1997. A new method to determine the zero-plane displacement. *Boundary-Layer Meteorology* 82: 159–164.

Dyer A.J. 1974. A review of flux-profile relationships. *Boundary-Layer Meteorology* 7: 363–372.

Foken T. 2006. 50 years of the Monin-Obukhov similarity theory. *Boundary-Layer Meteorology* 119: 431–447.

Foken T. & Wichura B. 1996. Tools for quality assessment of surface-based flux measurements. *Agricultural and Forest Meteorology* 78: 83–105.

Fuentes J.D., Wang D., Neumann H.H., Gillespie T.J., Hartog G. & Dann T.F. 1996. Ambient biogenic hydrocarbons and isoprene emissions from a mixed deciduous forest. *Journal of Atmospheric Chemistry* 25: 67–95.

Garratt J.R. 1980. Surface influence upon vertical profiles in the atmospheric near-surface layer. *Quarterly Journal of the Royal Meteorological Society* 106: 803–819.

Garratt J.R. 1994. *The atmospheric boundary layer*. Cambridge University Press, Cambridge and New York.

Ghirardo A., Koch K., Taipale R., Zimmer I., Schnitzler J.-P. & Rinne J. 2010. Determination of de novo and pool emissions of terpenes from four common boreal/alpine trees by $^{13}CO_2$ labelling and PTR-MS analysis. *Plant, Cell and Environment* 33: 781–792.

Goulden M.L., Daube B.C., Fan S.-M., Sutton D.J., Bazzaz A., Munger J.W. & Wofsy S.C. 1997. Physiological response of a black spruce forest to weather. *Journal of Geophysical Research* 102: 28987–28996.

de Gouw J. & Warneke C. 2007. Measurements of volatile organic compounds in the earth's atmosphere using proton-transfer-reaction mass spectrometry. *Mass Spectrometry Reviews* 26: 223–257.

Guenther A. 1997. Seasonal and spatial variations in natural volatile organic compound emissions. *Ecological Applications* 7: 34–45.

Guenther A.B., Monson R.K. & Fall R. 1991. Isoprene and monoterpene emission rate variability: observations with eucalyptus and emission rate algorithm development. *Journal of Geophysical Research* 96: 10799–10808.

Guenther A.B., Zimmerman P.R., Harley P.C., Monson R.K. & Fall R. 1993. Isoprene and monoterpene emission rate variability: model evaluations and sensitivity analyses. *Journal of Geophysical Research* 98: 12609–12617.

Guenther A.B., Karl T., Harley P., Wiedinmyer C., Palmer P.I. & Geron C. 2006. Estimates of global terrestrial isoprene emissions using MEGAN (model of emissions of gases and aerosols from nature). *Atmospheric Chemistry and Physics* 6: 3181–3210.

Guenther A.B., Kulmala M., Turnipseed A., Rinne J., Suni T. & Reissel A. 2011. Integrated land ecosystem-atmosphere processes study (iLEAPS) assessment of global observational networks. *Boreal Environment Research*

16: 321–336.

Guenther A.B., Hewitt C.N., Erickson D., Fall R., Geron C., Harley T.G.P., Klinger L., Lerdau M., McKay W.A., Pierce T., Scholes B., Tallamraju R.S.R., Taylor J. & Zimmerman P. 1995. A global model of natural volatile organic compound emissions. *Journal of Geophysical Research* 100: 8873–8892.

Hakola H., Héllen H., Hemmilä M., Rinne J. & Kulmala M. 2012. In situ measurements of volatile organic compounds in a boreal forest. *Atmospheric Chemistry and Physics* 12: 11665–11678.

Hari P. & Kulmala M. 2005. Station for measuring ecosystem–atmosphere relations (SMEAR II). *Boreal Environment Research* 10: 315–322.

Horst T.W. 1997. A simple formula for attenuation of eddy fluxes measured with first-order-response scalar sensors. *Boundary-Layer Meteorology* 82: 219–233.

Horst T.W. 1999. The footprint for estimation of atmosphere-surface exchange fluxes by profile techniques. *Boundary-Layer Meteorology* 90: 171–188.

Ibrom A., Dellwik E., Larsen S.E. & Pilegaard K. 2007. On the use of the Webb–Pearman–Leuning theory for closed-path eddy correlation measurements. *Tellus* 59B: 937–946.

Jiménez E., Lanza B., Martínez E. & Albaladejo J. 2007. Daytime tropospheric loss of hexanal and trans-2-hexenal: OH kinetics and UV photolysis. *Atmospheric Chemistry and Physics* 7: 1565–1574.

Kaimal J.C. & Finnigan J.J. 1994. *Atmospheric boundary layer flows: their structure and measurement*. Oxford University Press, New York.

Karl T., Guenther A., Jordan A., Fall R. & Lindinger W. 2001. Eddy covariance measurement of biogenic oxygenated VOC emissions from hay harvesting. *Atmospheric Environment* 35: 491–495.

Karl T., Spirig C., Rinne J., Stroud C., Prevost P., Greenberg J., Fall R. & Guenther A. 2002. Virtual disjunct eddy covariance measurements of organic compound fluxes from a subalpine forest using proton transfer reaction mass spectrometry. *Atmospheric Chemistry and Physics* 2: 279–291.

Kazil J., Stier P., Zhang K., Quaas J., Kinne S., O'Donnell D., Rast S., Esch M., Ferrachat S., Lohmann U. & Feichter J. 2010. Aerosol nucleation and its role for clouds and earth's radiative forcing in the aerosol-climate model ECHAM5-HAM. *Atmospheric Chemistry and Physics* 10: 10733–10752.

Kolari P., Bäck J., Taipale R., Ruuskanen T.M., Kajos M.K., Rinne J., Kulmala M. & Hari P. 2012. Evaluation of accuracy in measurements of VOC emissions with dynamic chamber system. *Atmospheric Environment* 62: 344–351.

Koppman R. 2007. *Volatile organic compounds in the atmosphere*. Blackwell Publishing Ltd., Oxford, UK.

Kulmala M., Suni T., Lehtinen K.E.J., Maso M.D., Boy M., Reissell A., Rannik Ü., Aalto P., Keronen P., Hakola H., Bäck J., Hoffmann T., Vesala T. & Hari P. 2004. A new feedback mechanism linking forests, aerosols, and climate. *Atmospheric Chemistry and Physics* 4: 557–562.

Kulmala M., Kontkanen J., Junninen H., Lehtipalo K., Manninen H.E., Nieminen T., Petäjä T., Sipilä M., Schobesberger S., Rantala P., Franchin A., Jokinen T., Järvinen E., Äijälä M., Kangasluoma J., Hakala J., Aalto P.P., Paasonen P., Mikkilä J., Vanhanen J., Aalto J., Hakola H., Makkonen U., Ruuskanen T., Mauldin R.L.III, Duplissy J., Vehkamäki H., Bäck J., Kortelainen A., Riipinen I., Kurtén T., Johnston M.V., Smith J.N., Ehn M., Mentel T.F., Lehtinen K.E.J., Laaksonen A., Kerminen V.-M. & Worsnop D.R. 2013. Direct observations of atmospheric aerosol nucleation. *Science* 339: 943–946.

Lenschow D.H., Mann J. & Kristensen L. 1994. How long is long enough when measuring fluxes and other turbulence statistics? *Journal of Atmospheric and Oceanic Technology* 11: 661–673.

Lindinger W., Hansel A. & Jordan A. 1998. On-line monitoring of volatile organic compounds at pptv levels by means of proton-transfer-reaction mass spectrometry (PTR-MS) — medical applications, food control and environmental research. *International Journal of Mass Spectrometry* 173: 191–241.

Massman W.J. & Lee X. 2002. Eddy covariance flux corrections and uncertainties in long-term studies of carbon and energy exchanges. *Agricultural and Forest Meteorology* 113: 121–144.

Mölder M., Grelle A., Lindroth A. & Halldin S. 1999. Flux-profile relationships over a boreal forest — roughness sublayer corrections. *Agricultural and Forest Meteorology* 98–99: 645–658.

Monin A.S. & Obukhov A.M. 1954. Basic laws of turbulent mixing in the atmosphere near the ground. *Trudy Geofiz. Inst*. 151(24): 163–187. [Translated by John Miller for Geophysics Research Directorate, AF Cambridge Research Centre, Cambridge, Massachusetts]

Moore C.J. 1986. Frequency response corrections for eddy correlation systems. *Boundary-Layer Meteorology* 37: 17–35.

Obukhov A.M. 1971. Turbulence in an atmosphere with a non-uniform temperature. *Boundary-Layer Meteorology* 2: 7–29.

Rannik Ü. 1998. On the surface layer similarity at a complex forest site. *Journal of Geophysical Research* 103: 8685–8697.

Rannik Ü., Keronen P., Hari P. & Vesala T. 2004. Estimation of forest–atmosphere CO_2 exchange by eddy covariance and profile techniques. *Agricultural and Forest Meteorology* 126: 141–155.

Rinne J., Bäck J. & Hakola H. 2009. Biogenic volatile organic compound emissions from Eurasian taiga: current knowledge and future directions. *Boreal Environment Research* 14: 807–826.

Rinne J., Guenther A.B., Warneke C., de Gouw J.A. & Luxembourg S.L. 2001. Disjunct eddy covariance technique for trace gas flux measurements. *Geophysical Research Letters* 28: 3139–3142.

Rinne J., Tuovinen J.-P., Laurila T., Hakola H., Aurela M. & Hypén H. 2000. Measurements of hydrocarbon fluxes by a gradient method above a northern boreal forest. *Agricultural and Forest Meteorology* 102: 25–37.

Rinne J., Taipale R., Markkanen T., Ruuskanen T.M., Héllen H., Kajos M., Vesala T. & Kulmala M. 2007. Hydrocarbon fluxes above a scots pine forest canopy: measurements and modeling. *Atmospheric Chemistry and Physics* 7: 3361–3372.

Rinne J., Markkanen T., Ruuskanen T.M., Petäjä T., Keronen P., Tang M.J., Crowley J.N., Rannik Ü. & Vesala T. 2012. Effect of chemical degradation on fluxes of reactive compounds — a study with a stochastic lagrangian transport model. *Atmospheric Chemistry and Physics* 12: 4843–4854.

Simpson I.J., Thurtell G.W., Neumann H.H., Hartog G.D. & Edwards G.C. 1998. The validity of similarity theory in the roughness sublayer above forests. *Boundary-Layer Meteorology* 87: 69–99.

Spanke J., Rannik Ü., Forkel R., Nigge W. & Hoffman T. 2001. Emission fluxes and atmospheric degradation of monoterpenes above a boreal forest: field measurements and modelling. *Tellus* 56B: 406–422.

Spirig C., Neftel A., Ammann C., Dommen J., Grabmer W., Thielmann A., Schaub A., Beauchamp J., Wisthaler A. & Hansel A. 2005. Eddy covariance flux measurements of biogenic VOCs during ECHO 2003 using proton transfer reaction mass spectrometry. *Atmospheric Chemistry and Physics* 5: 465–481.

Taipale R., Ruuskanen T.M. & Rinne J. 2010. Lag time determination in DEC measurements with PTR-MS. *Atmospheric Measurement Techniques* 3: 405–429.

Taipale R., Kajos M.K., Patokoski J., Rantala P., Ruuskanen T.M. & Rinne J. 2011. Role of *de novo* biosynthesis in ecosystem scale monoterpene emissions from a boreal scots pine forest. *Biogeoscience* 8: 2247–2255.

Taipale R., Ruuskanen T.M., Rinne J., Kajos M.K., Hakola H., Pohja T. & Kulmala M. 2008. Technical note: quantitative long-term measurements of VOC concentrations by PTR-MS — measurement, calibration, and volume mixing ratio calculation methods. *Atmospheric Chemistry and Physics* 8: 6681–6698.

Wienhold F.G., Frahm H. & Harris G.W. 1994. Measurements of N_2O fluxes from fertilized grassland using a fast response tunable diode laser spectrometer. *Journal of Geophysical Research* 99(D8): 16557–16568.